Received 20 June 2022 | Revised 07 July 2022 | Accepted 19 July 2022
Vol. 03, No. 01, 08 pages

RESEARCH ARTICLE

Tobruk University Journal of Engineering Sciences

Study Effect of Depth for Concrete Filled Steel Tubular Columns under Axial Load

Ibtisam. F. Abou-ajaila[1], Zuhiar A. Muhamed[2], Idress Saad[3], Mohamad Gabar[4]

[1,2] Department of Civil Engineering, Derna University, Alqubah, Libya
[3]Department of Roads and Ianding Engineering, Bright Star University, Brega, Libya
[4] Department of Civil Engineering, Tobruk University, Tobruk, Libya
`i.abouajaila@uod.edu.ly`

Abstract. The main purpose of this research is to study the effect of length on the CFT columns analytical using the finite element FE method. ANSYS software is employed to evaluate the CFT columns behavior. 3-D finite element models are presented and calibrated successfully to predict the CFT columns performance under axial static loading. A parametric study was conducted to evaluate the performance of CFT columns that examines the effect of all the dimensions of the CFT columns on the columns performance. The study considers varying the geometrical of the CFT columns, such as column width-to-thickness ratio and column length-to-width. The test results showed that increasing the slenderness ratio L/B has a negligible effect on the load capacity of the column but is accompanied by a large reduction of its ductility.

Keywords: Concrete-filled steel tube (CFT), ANSYS, Finite element method (FEM).

1 Introduction

Steel structural hollow sections are the most efficient of all the structural sections in resisting compression loads. Filling these sections with plain concrete significantly increases load-bearing capacity (Goode et al. [1]). CFT composite columns are usually categorized as either short or slender. These terms do not refer to the physical appearance or to the ratio of lateral dimensions to length, but rather to their modes of failure. If the load resistance is significantly reduced by second order moments, caused by column deflections, the column is classified as slender; otherwise it is classified as short. The load resistance of a short CFT column is governed by its section strength, which is the capacity of the cross-section to resist the applied axial loads and moments and is based purely on the material strength of the section. The load resistance of a slender CFT column is governed by what can be termed its member strength, reflecting the fact that the load resistance is dependent not only on the material properties, but also on the geometric properties of the entire member (Johansson, M. [2]). Many authors (Neogi et al. [3], Chen and Chen [4], Bridge [5] and Prion and Boehme [6]) have agreed that a slenderness ratio (L/D) equal to 15 generally marks a rough boundary between short and long column behavior. Knowles and Park [7] and AIJ [8] proposed an L/D value of 12, above which confinement does not occur. Both elastic and inelastic flexural buckling can occur in CFT columns. Ibrahim [9] mentioned CFT that fail by inelastic buckling are referred as intermediate CFT columns and CFT that fail by elastic buckling are referred to as long or slender CFT columns.

The failure of thick-walled short columns begins with the yielding of the steel. As the yielding of the cross-section of the tube proceeds, the concrete begins to fail by crushing. With confinement, the concrete can continue to sustain additional load until the steel tube fails (usually by extensive local buckling or full plastification of the cross-section) marking the ultimate strength of the section. The location of failure is usually mid-height for square and rectangular CFT specimens. For square CFT, local buckling generally spreads to all four flanges. However, for rectangular CFT, the longer flanges are more susceptible to local buckling. This causes steel yielding in the transverse direction along the shorter sides (Shakir-Khalil [10]). O'Shea and Bridge [11] showed that the concrete infill for the thin-walled circular steel tubes has little effect on the local buckling strength of the steel tubes. However, O'Shea and Bridge [12] found that concrete infill can improve the local buckling strength for rectangular and square sections.

Increased strength due to confinement of high-strength concrete can be obtained if only the concrete is loaded and the steel is not bonded to the concrete. Therefore, they considered that the strength of these sections can be estimated using Eurocode 4 [13] with confinement ignored. The mode of failure of long concrete filled steel tube columns is characterized by overall elastic buckling of the member (Shakir- Khalil and Zeghiche [14]). This type of column has a sufficiently large L/D ratio to cause buckling before any significant yielding occurs in the column. Tsuda et al. [15] observed the same type of failure in their tests of slender concentrically loaded columns. The columns with an L/D greater than 18 did not reach their plastic axial strength and failed by flexural buckling. The aim of this work is to employ the nonlinear finite element (FE) program ANSYS [16] to perform numerical simulations of CFT columns subjected to axial loads. The parametric study is conducted using 9 specimens under concentric compression for square CFT columns. The primary parameters considered in this study include for columns: column width-to-thickness B/t and column depth-to- width L/B.

2 Finite Element Model

The FE method has been extensively used to study the structural behaviors of steel-concrete composite section. The well-known commercial finite element package, (ANSYS V10) is employed in the present study. 3-D FE model is developed in order to predict the performance of the CFT columns under static loading. The issue concerning in modeling a problem using the FEM is described. The different finite element types used in the modeling of CFT columns are:

Steel Plate Element (Shell 181): (4-node plastic large strain shell): is used to model both the steel tube.

Concrete Element (Solid 65): (8-node 3-D structural solid): is used to model concrete core.

Contact between Steel and Concrete (Targe 170 and Conta 173): (3-D point-point contact element): is used to model the connection between concrete core and steel tube. Both target and contact elements are paired via a shared real constant. When the two surfaces are in contact, a frictional force is resulted. A friction coefficient between steel tube and concrete core is used as 0.25 (Hu et al.[17]). Meshing is one of the most important issues in modeling since the accuracy of the results largely depends on it. The technique of FE lies in the development of a suitable mesh arrangement. The meshing process must balance the need for a fine mesh to give an accurate stress distribution and reasonable analysis time.

The optimal solution is to use a fine mesh in areas of high stress and a coarser mesh in the remaining areas. Fig. 1 shows the finite element mesh of an analyzed CFT column. The mesh has to be relatively coarse based on the studies of Hu et al.[17] who recognized that the mesh refinement has very little influence. Due to symmetry, symmetric boundary conditions are enforced on the symmetric planes, for which u=0 and w=0 on the planes normal to the x and z-axis respectively. According to the mechanism of loading and test setup, the boundary conditions of the analyzed columns are both ends allow rotations in the whole directions as shown in Fig. 1. Column upper end allows a displacement in y-direction (direction of the column axis) only while the lower end does not allow any displacements.

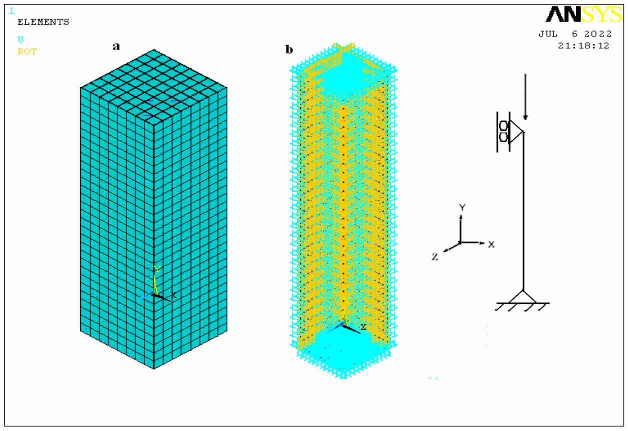

Fig.1. General view of the column. (a) meshing of model. (b) symmetry of model, and boundary condition.

3 Material Modeling

The stress strain relationships for concrete core and steel plates were idealized for the finite element model as described below:

3.1 Steel Tube

The uniaxial behavior of the steel tube can be simulated by an elastic-perfectly plastic model as shown in Fig. 2 When the stress points fall inside the yield surface, the behavior of the steel tube is linearly elastic. If the stresses of the steel tube reach the yield surface, the behavior of the steel tube becomes perfectly plastic. Consequently, the steel tube is assumed to fail and cannot resist any further load (Hu et al.[18]). The modulus of elasticity for steel (Es) is taken as 200000 MPa, poisson's ratio is assumed to be νs = 0.3 (Hu et al.[18]).

3.2 Concrete Material

The poisson’s ratio of concrete is assumed to be νc = 0.2, according to Dalin Liu [19], suggested the following equations to model the stress-strain curve of the concrete as shown in Fig. 3:

$$\sigma_C = E_C\,\varepsilon \qquad \text{for} \qquad \varepsilon \le \varepsilon_1 \tag{1}$$

$$\sigma_C = f_0 \qquad \text{for} \qquad \varepsilon_1 \le \varepsilon \le \varepsilon_2 \tag{2}$$

$$\sigma_C = f_0(\varepsilon_2/\varepsilon_1)^{0.24+0.45/\zeta} \qquad \text{for} \qquad \varepsilon \ge \varepsilon_2 \tag{3}$$

In which, $f_0 = 0.85 f_c^{\eta}$ (4)

$$\eta = 1 + \frac{\left(1-0.65(H/B-1)^3\right)\left(0.37\zeta^{0.82}-0.19\zeta\right)}{1+0.05(f'_C/50)^{5.65}} \tag{5}$$

$$\zeta = \frac{A_S\,f_y}{0.85 A_C f'_C} \tag{6}$$

$$\varepsilon_1 = f_0/E_C \tag{7}$$

$$\varepsilon_2 = 2\varepsilon_1 \tag{8}$$

The initial modulus of elasticity of concrete *c E* is highly correlated to its compressive strength and can be calculated with reasonable accuracy from the equation given in ACI code [20] as:

$$E_C = 4700\sqrt{f'_{cc}} \quad \text{MPa} \tag{9}$$

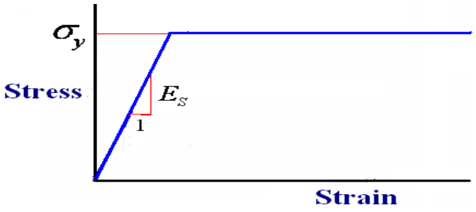

Fig. 2. Elastic-perfectly plastic model for steel tube (Hu et al. [18]).

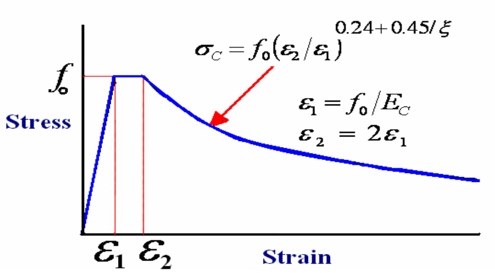

Fig. 3. Relationship for confined concrete.

4 Verification of the Model

Before the parametric study could be carried out, it was necessary to prove that the established finite element model is capable of simulating the structural behavior of CFT steel columns in order to give the coming parametric study intensity and reliability. The proposed finite element model is examined through comparisons with experimental work available in the literature. Comparing the results from ANSYS models with the published papers showed an accepted difference for the compared values up to 5%. The details of the verifications are briefly discussed in Rabie and Ibtisam et al. [21].

5 Parametric Study

A finite element models were constructed to simulate and compare between CFT columns. In this paper, the proposed model is extended to investigate the effect of length on the ultimate capacities and ductility of CFT columns. The parametric study is conducted using nine CFT box columns. The test specimens were slender and all the columns were square have the same width (B) of 200 mm. The dimensions of steel plate tube are the parameters to be examined. The parameters are put in a non-dimensional form where for columns: B/t and L/B. To get practical results, the values of non-dimensional parameters are taken in the range of previous experimental work mentioned in the literature, where; B/t varies between 50 and 100 and L/B varies between 14 and 30. The yield strength of steel, $f_y = 240$ MPa and concrete compressive strength, $f_C = 25$ MPa as listed in Table 1.

Table 1. Dimensions and material properties of CFT.

CFT columns	Column dimensions (mm)			Ratio		Material properties (MPa)	
	L	B	t	L/B	B/t	f_C	f_y
C1	2800	200	4	14	50	25	240
C2			3		67		
C3			2		100		
C4	4000		4	20	50		
C5			3		67		
C6			2		100		
C7	6000		4	30	50		
C8			3		67		
C9			2		100		

6 Ductility Factor (μ_{95})

The ductility definition proposed by Ge and Usami [22] is considered herein;

$$\mu_{95} = \partial_{95}/\partial_y \tag{10}$$

Where ∂_{95} =deformation corresponding to a load of 95% of the ultimate load at the side of descending part which is larger than the deformation corresponding to the ultimate load, and ∂_y is the yield displacement as shown in Fig. 4.

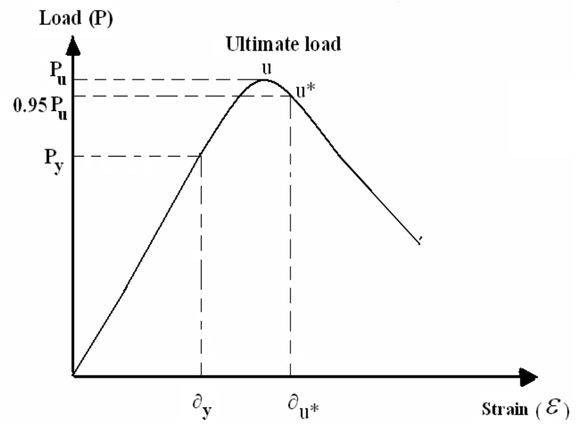

Fig. 4. Definition of ductility factor (μ_{95}).

7 Results and Discussion

Table 2 list the ultimate load capacities and the ductility factor (μ_{95}) of the analyzed CFT columns for different B/t and L/B ratios. Figs. 5 to 9 represent the results curves of the analyzed CFT columns for different ratios of studied parameters. Figs. 5 to7 indicate that increasing the B/t ratio, the load capacity as well as ductility of the column decreases.

According to Table 2 and for L/B=14, when B/t ratios increased by 34% and 100%, the ultimate axial load for an unstiffened column is decreased by 11% and 23%, respectively. On the other hand, the ductility factor for column decreased by 3% and 14% respectively.

Comparing Fig. 5 (L/B=14) and Fig. 6 (L/B=20) and also, Fig. 7 (L/B=30), one can realize that increasing the slenderness ratio L/B has a negligible effect on the load capacity of the column but is accompanied by a large reduction of its ductility. This result is in agreement with the conclusions made by Farage and Elhwiety [23]. Also, Fig. 7 indicate that when the column became very slender (L/B=30), then the columns had almost no ductility and sudden failure occurred in all the columns.

According to Fig. 8, it results in considerable decrease in the ductility factor (μ_{95}). As an example, when L/B ratio increased from 14 to 30, the ductility factor (μ_{95}) is decreased by 23%. Fig. 9 and Table 2, show that the increase in L/B ratios (increasing column length L) results in considerable decrease in the ductility factor (μ_{95}). As an example, when is obvious that in the elastic zone, there is no effect for the change of column length in both the stiffness and the strength of the CFT columns. The effect of length only appears in the post buckling zone. In this stage, increasing the column length decreases the ductility of the CFT columns. Increasing the length more than a certai), show that the increase in L/B ratios (increasing column length L) L/B ratio increased from 14 to 30 for an unstiffened column, the ductility factor (μ_{95}). is decreased by 23%.

Table 2. Results of ultimate capacity load and ductility factor.

CFT columns	Ratio		Ultimate capacity load (KN)	Ductility factor
	L/B	B/t		
C1	14	50	2080	1.59
C2		67	1844	1.54
C3		100	1600	1.36
C4	20	50	2088	1.36
C5		67	1820	1.32
C6		100	1580	1.29
C7	30	50	2088	1.29
C8		67	1804	1.28
C9		100	1560	1.27

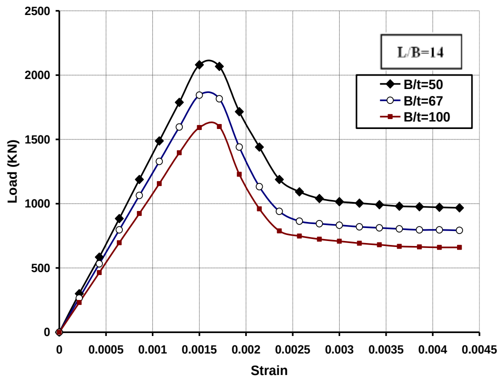

Fig. 5. Axial load-strain relationship for L/B=14 and different B/t ratios.

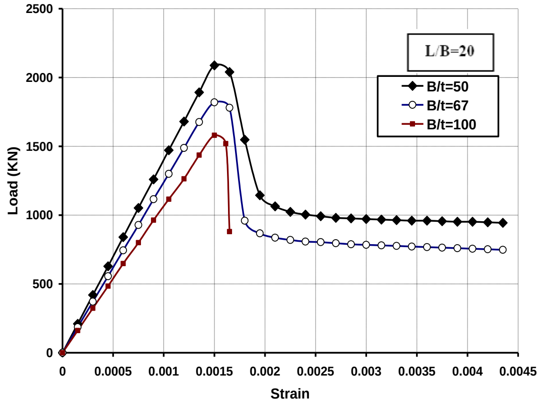

Fig. 6. Axial load-strain relationship for L/B=20 and different B/t ratios

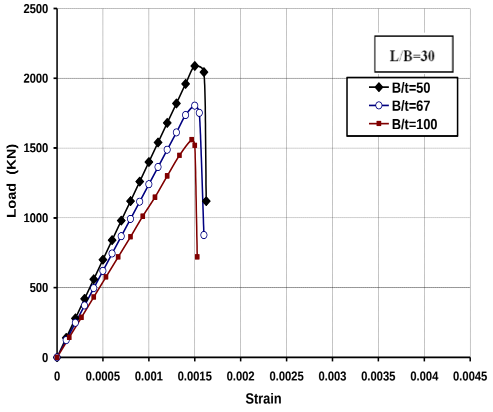

Fig. 7. Axial load-strain relationship for L/B=30 and different B/t ratios.

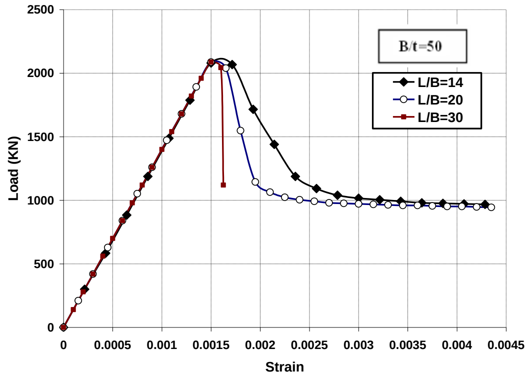

Fig. 8. Effect of column length for B/t=50.

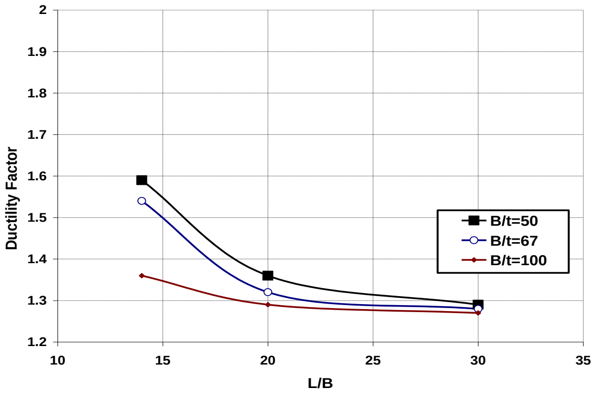

Fig. 9. Ductility factor (μ_{95}) - L/B ratio relationship for different B/t ratios.

8 Conclusions

This study presents a finite element model to estimate the axial behavior of box CFT columns under concentric axial loads. A numerical parametric study is conducted to study the influence of the tow parameters controlling the behavior of CFT columns. From the results obtained, it can be concluded that:

- Increasing B/t ratio leads to decreasing on both axial capacity and ductility of CFT columns. Such conclusion reflects the little contribution of the steel tube to the confinement as its thickness decreases.
- L/B ratio has no significant effects on the behavior of CFT columns. It has no effect upon both the stiffness and strength. However, increasing L/B ratio much decreases the column ductility.

Conflict of Interest

This is to certify that all authors have seen and approved the manuscript being submitted and to declare that they have no conflicts of interest.

References

1. Goode. D. C., Kuranovas. A., and Kvedaras. K. A. (2010). (Buckling of slender composite concrete filled steel columns). Journal of Civil Engineering and Management, Vol. 16, No. 2, pp. 230-236. Received 30 Oct. 2009; Accepted 11Feb. 2010.
2. Johansson, M. (2002). (Composite action and confinement effects in tubular steel-concrete columns). Licentiate thesis, Chalmers University of Technology, Department of Structural Engineering Sweden.
3. Neogi, p. k., Sen, H. K., and Chaprnan, J. C. (1969). (Concrete filled tubular steel columns under eccentric loading). The Structural Engineering, Vol. 47, No. 5, May 1969, pp. 187-195.
4. Chen, W. F., and Chen C. H. (1973). (Analysis of concrete-filled steel tubular beam-columns). IABSE Publications, Vol. 33, No. II, pp. 37-52.
5. Bridge, R. Q. (1976). (Concrete filled steel tubular columns). Civil Engineering Transactions, the Institution of Engineers, Australia, CE18 (2), pp. 127-133.
6. Prion, H. G. L., and Boehme, J. (1989). (Beam-column behavior of steel tubes filled with high strength concrete). Proceedings of the Fourth International Colloquium, Structural Stability Research Council, New York, pp.439-450.
7. Knowles, R. B., and park, R. (1969). (Strength of concrete filled steel tubular columns). Journal of the Structural Division, ASCE, Vol. 95, No. 12, pp. 2565-2587.
8. Architectural Institute of Japan (AIJ) (1997). (Recommendations for design and construction of concrete filled steel tubular structures). Tokyo, Japan.

9. Ibrahim, M. S. (2006). (Behavior of box steel columns filled with concrete under cyclic loading). Thesis No. 4149 library Alexandria University, Egypt.
10. Shakir Khalil, H. (1991). (Tests on concrete-filled hollow section columns). Proceedings of the Third International Conference on Steel-Concrete Composite Structures, Wakabayashi, M. (ed.)m Fukuoka, Japan, September 26-29, 1991, Association for International Cooperation and Research in Steel-Concrete Composite Structures, pp. 89-94.
11. O’Shea, M., and Bridge R. (1996). (Circular thin-walled tubes with high strength concrete infill). Composite Construction in Steel and Concrete II, ASCE, pp. 780–793.
12. O’Shea, M., and Bridge R. (1997). (The design for local buckling of concrete filled steel tubes). Composite Construction Conventional and Innovate, Innsbruck, Austria, pp. 319–324.
13. Eurocode 4, ENV 1994-1-1: 2004. Design of composite steel and concrete structures. Part 1.1: General rules and rules for buildings. London; 1994.
14. Shakir Khalil, H., and Zeghiche, Z. (1989). (Experimental behavior of concrete filled rolled rectangular hollow-section columns). The Structural Engineering, Vol. 67, No. 19, pp.345-353.
15. Tsuda, K., Matsui, C., and Mino, E. (1996). (Strength and behavior of slender concrete filled steel tubular columns). Stability Problems in Designing, Construction and Rehabilitation of Metal Structures, Proccedings of the Fifth International Colloquium on Structural Stability, SSRC IC/BRASIL ’96, Rio de Janerio, Brasil, August 5-7, Structural Stability Research Council, Bethlehem, Pennsylvania, pp. 489-500.
16. ANSYS 10.0 complete user’s manual set. Downloaded from http://www1.ansys.com/customer/content/documentation/100/ansys/readme.htm1.
17. Hu, H. T., Huang, C. S., Wu, M. H., and Wu, Y. M. (2002). (Numerical analysis of concrete-filled steel tubes subjected to axial force). Proceedings of the International Workshop on Steel and Concrete Composite Construction, National Center for Research on Earthquake Engineering, National Taiwan University, China.
18. Hu, H. T., Huang, C. S., Wu, M. H., and Wu, Y. M. (2003). (Nonlinear analysis of axially loaded concrete-filled tube columns with confinement effect). Journal of Structural Engineering, ASCE, Vol. 129, No. 10, pp. 1322-1329.
19. Dalin Liu. (2005). (Behavior of eccentrically loaded high strength rectangular concrete filled steel tubular columns). Journal of Constructional Steel Research, 2006 Vol. 62, PP. 839-846.
20. American Concrete Institute (ACI) (2002). (Building code requirements for structural concrete and commentary). ACI 318-02, Detroit.
21. Rabie. A. Amnisi, Ibtisam. F. ABOU-AJAILA and Maryam. E. Darwish. (2022). (Comparison Between Analytical and Experimental Methods for Concrete Filled Steel Tubular Columns), Albahit journal of applied sciences ISSN2708=244X, e=ISSN 2708-8936, Vol.3, Issue 1, pp. 41- 48.
22. Ge, H. B., and Usami, T. (1996). (Cyclic tests of concrete-filled steel box columns), Journal of Structural Engineering, Vol. 122, No. 10, pp. 1169–1177.
23. Farag, E. S., Elhwiety, M. M., Abo Elfath, H., and Mashaly, E. (2012). (Performance of concrete filled partially steel slender columns under axial load). M. SC. Thesis. Alexandria University, Structural Engineering Department, Egypt.